Comparative Medicine
Copyright 2006
by the American Association for Laboratory Animal Science

Vol 56, No 1
February 2006
Pages 68-74

Comparative Anatomy of Rabbit and Human Achilles Tendons with Magnetic Resonance and Ultrasound Imaging

Geoffrey P Doherty,[1] Yoichi Koike,[2] Hans K Uhthoff,[2,4] Martin Lecompte,[1] and Guy Trudel[2,3,*]

We sought to describe the comparative anatomy of the Achilles tendon in rabbits and humans by using macroscopic observation, magnetic resonance imaging, and ultrasonography. The calcaneus–Achilles tendon–gastrocnemius–soleus complexes from 18 New Zealand white rabbits underwent ultrasound (US) and magnetic resonance (MR) imaging and gross anatomic sectioning; these results were compared with those from a cadaveric gastrocnemius–soleus–Achilles tendon–calcaneus specimen from a 68-y-old human male. The medial and lateral gastrocnemius muscle tendons merged 5.2 ± 0.6 mm proximal to the calcaneal insertion macroscopically, at 93% of their course, different from the gastrocnemius human tendons, which merged at 23% of their overall course. The rabbit flexor digitorum superficialis tendon, corresponding to the flexor digitorum longus tendon in human and comparable in size with the gastrocnemius tendons, was located medial and anterior to the medial gastrocnemius tendon proximally and rotated dorsally and laterally to run posterior to the Achilles tendon–calcaneus insertion. In humans, the flexor digitorum longus tendon tracks posteriorly to the medial malleolus. The soleus muscle and tendon are negligible in the rabbit; these particular comparative anatomic features in the rabbit were confirmed on the MR images. Therefore the rabbit Achilles tendon shows distinctive gross anatomical and MR imaging features that must be considered when using the rabbit as a research model, especially for mechanical testing, or when generalizing results from rabbits to humans.

Abbreviations: FOV, field of view; MR, magnetic resonance; NEX, number of excitations; TE, echo time; TR, recovery time; PD, proton density; TSE, turbo spin echo; US, ultrasound

The Achilles tendon, also referred to as the calcaneal or calcanean tendon, is one of the most commonly injured sites in the lower limb.[13,27] Research into Achilles tendon injury, surgery, and repair relies heavily on animal models, including rats,[9] dogs,[17,26] cats,[17] and rabbits.[2,3,5,9,12,14,15,18,21,29,30] The rabbit has been used widely for Achilles tendon research because it is commonly available and the size of the Achilles tendon is suitable for both histologic assessment and mechanical testing.[14,21,29,30]

Compared with human anatomy (Figure 1), some peculiarities of the rabbit leg are known, such as the absence of the flexor digitorum longus tendon as well as the presence of the flexor digitorum superficialis tendon.[4,24] However, those peculiarities have never been described in terms of relationship to the Achilles tendon, nor have they been studied with imaging modalities.

We proposed to document the anatomy around the Achilles tendon in the rabbit and correlate gross pathologic sections with both magnetic resonance (MR) and ultrasound (US) imaging. Our objectives were to describe the anatomic relationship between the Achilles and flexor digitorum superficialis tendons and to clarify the appearance of those tendons on both MR and US imaging.

Materials and Methods

Materials. The protocol for these experiments was approved by the University of Ottawa Ethics Committee, adhering to guidelines set forth from the institutional animal care and use committee. One right gastrocnemius–soleus–Achilles tendon–calcaneus unit from a 68-y-old man was harvested postmortem for macroscopic observation and MR and US imaging. Eighteen adult female New Zealand White rabbits (*Orytolagus cuniculus*; average weight, 2.6 kg; Charles River Canada, Saint-Constant, Quebec, Canada) were used and singly housed in stainless steel rabbit racks (Ancare, Bellmare, NY). These animals were used later in a study of mechanical properties of the rabbit Achilles tendon. Animals were euthanized with overdoses of pentobarbital (100 mg/kg intravenously) and bilateral gastrocnemius–soleus–Achilles tendon–calcaneus complexes were resected en bloc. Each specimen then was wrapped in gauze, moistened in saline solution without fixation, and stored at –13 °C until imaging.

Magnetic resonance imaging. At the time of testing, the specimens were allowed to thaw gradually to room temperature. The tendons were aligned and imaged in groups of 6 in a specially designed box (Figure 2). MR imaging was performed using a Symphony 1.5 T MR unit (Siemens Medical Systems, Iselin, NJ) and its extremity coil. The human Achilles tendon was imaged with the axial proton density (PD) dual echo (recovery time [TR], 3000 ms; echo time [TE], 15 ms, field of view [FOV], 130 mm; matrix, 512 × 512, number of excitations [NEX], 1; slice thickness, 3 mm), axial T1 spin echo (TR, 513 ms; TE, 12 ms; FOV, 130 mm; matrix, 512 × 512; NEX, 2; slice thickness, 3 mm), and sagittal T1 spin echo (TR, 3490 ms; TE, 15 ms; FOV, 130 mm; matrix, 512 × 512; NEX, 2; slice thickness, 2 mm) sequences. For the rabbit specimens, axial

Received: 7 Mar 2005. Revision requested: 25 Aug 2005. Accepted: 7 Dec 2005.
[1]Department of Radiology, [2]The Bone and Joint Research Laboratory, [3]Department of Medicine, Division of Physical Medicine and Rehabilitation, and [4]Faculty of Medicine, University of Ottawa.
[*]Corresponding author. Email: gtrudel@ottawahospital.on.ca

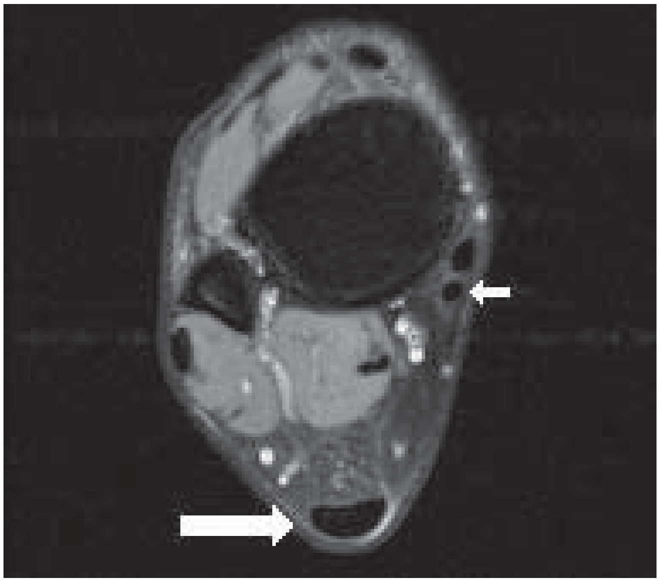

Figure 1. MR image of human Achilles and flexor digitorum longus tendons. The Achilles tendon is in the posterior compartment (large arrow) on an axial T2 TSE image with fat saturation. The flexor digitorum longus muscle runs in the deep-posterior compartment, and its tendon runs posterior the medial malleolus (small arrow).

images were obtained with T1 spin echo (TR, 400 ms; TE, 14 ms; FOV, 130 mm; matrix, 640 × 640, NEX, 2; slice thickness, 3 mm) and dual echo (PD and T2-weighted images) turbo spin echo (TSE) (TR, 4680 ms; TE, 15 and 87 ms; FOV, 130 mm; matrix, 640 × 640; NEX, 2; slice thickness, 3 mm) acquisitions. Sagittal images were obtained with T1 spin echo (TR, 428 ms; TE, 14; FOV, 130 mm; matrix, 512 × 512; NEX, 2; slice thickness, 2 mm), PD TSE (TR, 2720 ms; TE, 20; FOV, 130 mm; matrix, 512 × 512; NEX, 2; slice thickness, 2 mm), and sagittal T2 TSE (TR, 3050 ms; TE, 20 ms; FOV, 130 mm; matrix, 512 × 512; NEX, 2; slice thickness, 2 mm) acquisitions. The maximal anteroposterior measurements of each medial and lateral gastrocnemius tendons and flexor digitorum superficialis tendon were obtained at 15 mm proximal to the Achilles tendon–calcaneus insertion, using measuring tools for Horizon Rad Station imaging software (version 3.3, McKesson, San Francisco, CA); and means and standard deviations were calculated.

Ultrasonography. US images of the human and rabbit Achilles tendons were captured using a HDI 5000 unit (Philips Medical Systems, Markham, Ontario, Canada). Axial images were obtained at 5-mm intervals, starting at the calcaneal insertion and proceeding 8 cm proximally in the human and 3.5 cm proximally in the rabbit, by using a compact linear-array transducer (CL10-5, Philips Medical Systems). Three sagittal images—at the medial, midpoint, and lateral aspects of the tendon—were obtained with a linear-array 50-mm transducer (L12-5, Philips Medical Systems).

The maximal anteroposterior measurement of the human Achilles tendon was calculated. Measurements of maximal anteroposterior dimension of rabbit tendons were planned but not obtained, as individual tendons could not be identified clearly in either the axial or sagittal plane.

Macroscopic observation. After imaging of the rabbit specimens, Achilles tendons were observed macroscopically, and the anatomic relationships of the tendons of medial and lateral gastrocnemius, soleus, and flexor digitorum superficialis were

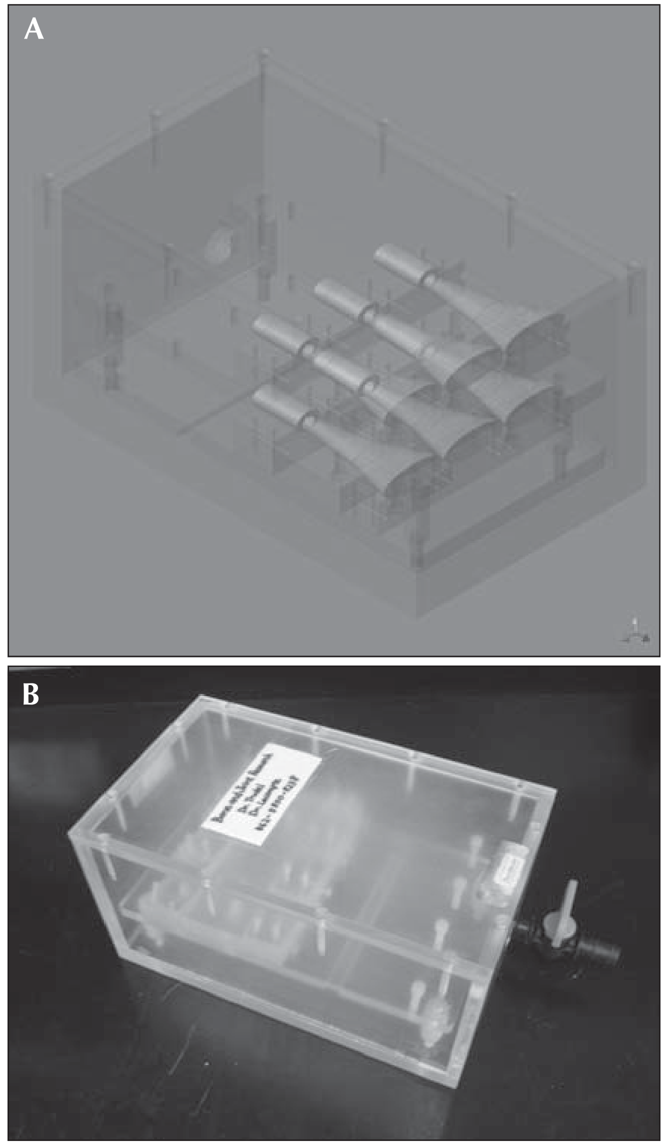

Figure 2. The waterproof, 2-story, acrylic box designed to image rabbit Achilles tendons accommodated 6 rabbit Achilles tendons attached to their calcanei and aligned them in the same plane. The acrylic box, plastic screws, and rubber seals did not interfere with US and MR imaging. The box was filled with saline solution for imaging. (A) Schematic representation of the box containing 6 rabbit tendons. (B) Photograph of the box actually used.

recorded. The point at which the lateral and medical gastrocnemius tendons merged to form the common Achilles tendon was measured with calipers in reference to the calcaneal insertion. The calcaneus–Achilles tendon–gastrocnemius–soleus complex was sectioned in the transverse plane at 0, 2, 5, 7, 10, 12, 15, 17, 20, and 22 mm from the calcaneal insertion, and sections were fixed in formaldehyde for 2 wk.

Results

Gross anatomy. In the human sample, the medial and lateral heads of the gastrocnemius muscle converged 200 mm proximal to the calcaneal insertion, at 23% of their course to the Achilles

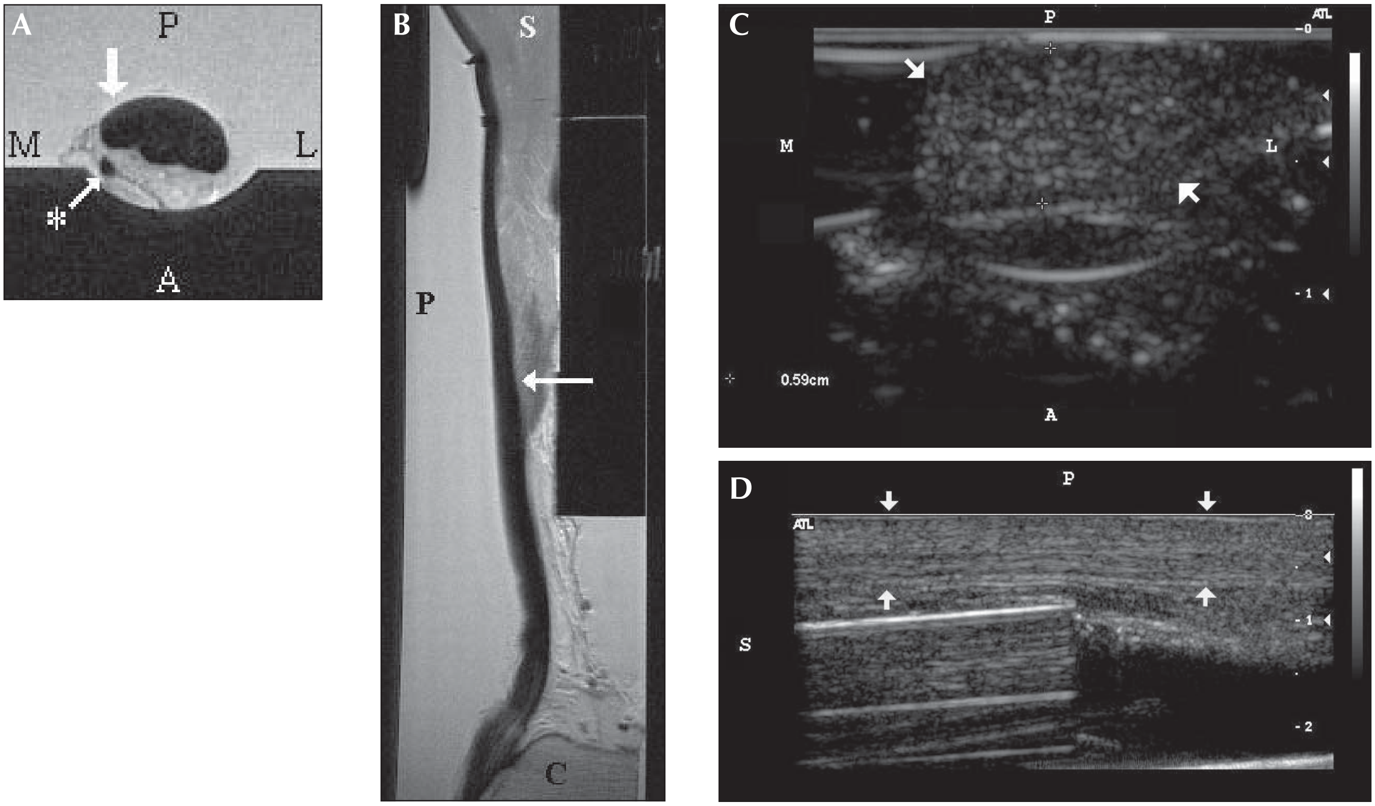

Figure 3. MR and US images of a cadaveric human Achilles tendon. (A) The Achilles tendon (white arrow) on an axial PD image. The plantaris tendon (*) runs medial to the Achilles tendon. A, anterior; P, posterior; M, medial; L, lateral. (B) The Achilles tendon (white arrow) on a sagittal PD image. S, superior; P, posterior; C, calcaneus. (C) The Achilles tendon (white arrow) on an axial US image. A, anterior; P, posterior; M, medial; L, lateral. (D) The Achilles tendon (white arrow) on a sagittal (D) US image. S, superior; P, posterior.

tendon insertion (the total length of gastrocnemius muscle–soleus muscle–Achilles tendon complex was 260 mm). The mass of gastrocnemius–soleus muscle provided fibers to form the Achilles tendon, which rotated externally as they tracked distally. The Achilles tendon was accompanied only by the plantaris tendon in the posterior compartment. The flexor digitorum longus muscle was in the deep-posterior compartment, and its tendon ran behind the medial malleolus (Figure 3).

In all 18 rabbits, the anatomic relationships between the tendons of the medial and lateral gastrocnemius, soleus, and flexor digitorum superficialis were found to be consistent and reproducible. The flexor digitorum superficialis tendon was located medially and anterior to the medial gastrocnemius tendon (Figure 4). The lateral gastrocnemius tendon, to which there was negligible contribution from the soleus muscle, was located anterolateral to the medial gastrocnemius muscle.

As the medial gastrocnemius tendon tracked distally, it rotated laterally to become posterior in relationship to the lateral gastrocnemius tendon. The medial and lateral gastrocnemius muscles each provided fibers to the rabbit Achilles tendon. These fibers converged only 5.2 ± 0.6 mm (mean ± 1 standard deviation) proximal to the Achilles tendon–calcaneal insertion, at 93% of the overall course to the Achilles tendon insertion (the total length of the gastrocnemius–soleus–Achilles complex, from muscle origin proximally to tendon insertion distally, measured 70.0 ± 10.0 mm). The flexor digitorum superficialis tendon tracked medially and posteriorly, in relation to the medial and lateral head of gastrocnemius components, and inserted posteriorly to the Achilles tendon at the calcaneus. At this level, it shared the same sheath as the Achilles tendon. At the level of the calcaneus, the flexor digitorum superficialis tendon was positioned immediately posterior to the Achilles tendon–calcaneus insertion (Figure 4).

MR imaging. The human Achilles tendon was accompanied only by the plantaris tendon in the posterior compartment (Figure 3). The flexor digitorum longus muscle ran in the deep-posterior compartment, and its tendon tracked posterior to the medial malleolus. The anteroposterior dimension of the Achilles (6.7 mm) was much larger than that of the flexor digitorum longus tendon (1.3 mm).

The rabbit Achilles, medial and lateral gastrocnemius, and flexor digitorum superficialis tendons have low signal intensity on all imaging sequences. The particular gross anatomic relationships of these tendons were confirmed on the MR images. The soleus muscle was not detected in the axial or sagittal plane. In the 3-mm cross-sectional images, the 2 gastrocnemius tendons were seen distinctly as they tracked inferiorly from their respective muscles (Figure 4). At 15 mm proximal to the Achilles tendon–calcaneus insertion, the anteroposterior dimension of the flexor digitorum superficialis tendon (1.7 ± 0.1 mm) was comparable to those of the tendons of the medial (1.7 ± 0.1 mm) and lateral (1.8 ± 0.1 mm) heads of the gastrocnemius muscles (Figure 4). The combined Achilles tendon (2.1 ± 0.1 mm) was visualized only on the images taken approximately 3 mm from the calcaneal insertion. On sagittal images, the individual tendons were difficult to separate due to rotation of the medial and lateral gastrocnemius and flexor digitorum superficialis

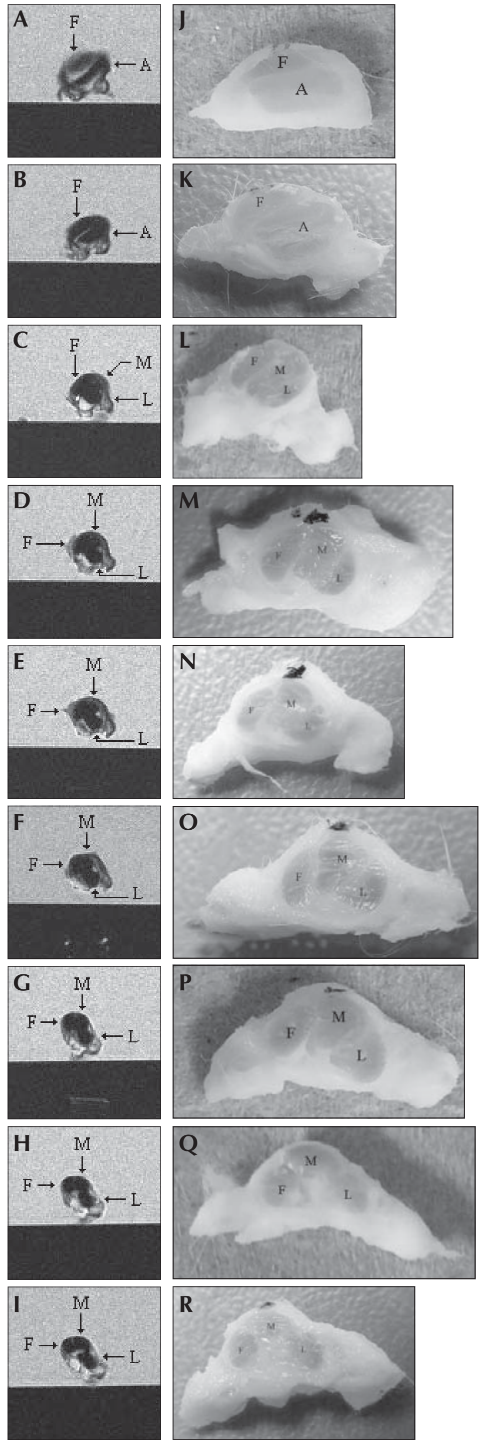

Figure 4. Axial PD MR images (left panels) and axial gross anatomy sections (right panels) of the rabbit calcaneus–Achilles tendon–gastrocnemius–soleus complex. F, flexor digitorum superficialis tendon; M, medial gastrocnemius tendon; L, lateral gastrocnemius tendon; A, Achilles tendon. (A) Axial PD MR image at 0 mm proximal to the calcaneus. (B) Axial PD MR image at 3 mm proximal to the calcaneus. (C) Axial PD MR image at 6 mm proximal to the calcaneus. (D) Axial PD MR image at 9 mm proximal to the calcaneus. (E) Axial PD MR image at 12 mm proximal to the calcaneus. (F) Axial PD MR image at 15 mm proximal to the calcaneus. (G) Axial PD MR image at 18 mm proximal to the calcaneus. (H) Axial PD MR image at 21 mm proximal to the calcaneus. (I) Axial PD MR image at 24 mm proximal to the calcaneus. (J) Transverse cross-section gross anatomy image at 0 mm proximal to the calcaneus. (K) Transverse cross-section gross anatomy image at 2 mm proximal to the calcaneus. (L) Transverse cross-section gross anatomy image at 5 mm proximal to the calcaneus. (M) Transverse cross-section gross anatomy image at 10 mm proximal to the calcaneus. (N) Transverse cross-section gross anatomy image at 12 mm proximal to the calcaneus. (O) Transverse cross-section gross anatomy image at 15 mm proximal to the calcaneus. (P) Transverse cross-section gross anatomy image at 17 mm proximal to the calcaneus. (Q) Transverse cross-section gross anatomy image at 20 mm proximal to the calcaneus. (R) Transverse cross-section gross anatomy image at 22 mm proximal to the calcaneus.

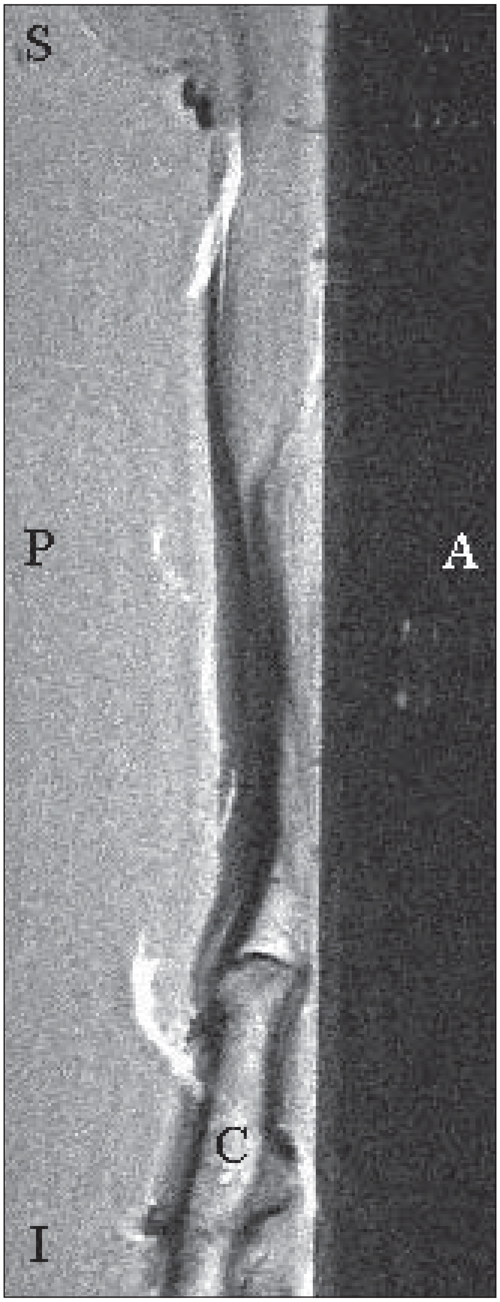

Figure 5. Sagittal PD MR image of the rabbit calcaneus–Achilles tendon–gastrocnemius–soleus complex. S, superior; I, inferior; A, anterior; P, posterior; C, calcaneus.

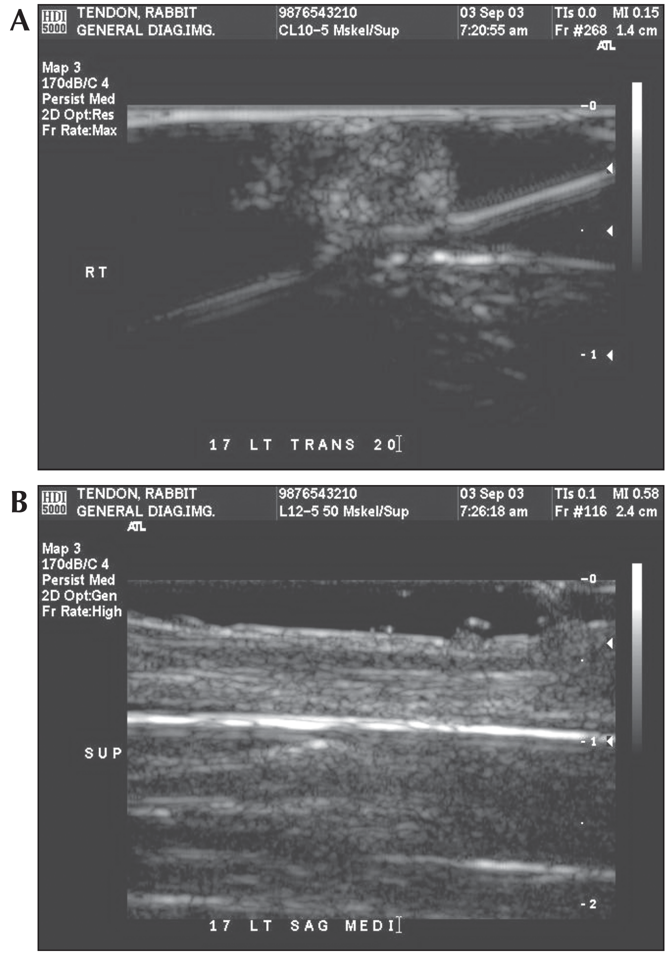

Figure 6. Axial (A) and sagittal (B) US image samples of a rabbit calcaneus–Achilles tendon–gastrocnemius–soleus complex. The axial image is of a left leg at 20 mm proximal to the calcaneal insertion of the Achilles tendon; RT, right. The sagittal image was obtained approximately at midsection; SUP, superior.

tendons (Figure 5).

US imaging. The maximal anteroposterior dimension of the human Achilles tendon measured 5.9 mm.

Transverse US images of the rabbit calcaneus–Achilles tendon–gastrocnemius–soleus complex were obtained but were technically difficult to interpret due to the extensive anisotropy caused by the 3 distinct sets of tendon fibers tracking in different orientations. The axial plane did not yield conclusive images for identifying or measuring each muscle and tendon (Figure 6). Sagittal images did show tendon fibers, but again, the anisotropy and small dimension made accurate identification impossible.

Discussion

The human Achilles is the most commonly injured tendon in the lower leg.[13,27] The rabbit has been used widely for Achilles tendon research.[2,3,5,8,12,14,15,18,21,29,30] Knowledge of the anatomy of Achilles tendon in rabbits is important for planning experimental research and generalizing the results to human problems. Here we describe the unique anatomy of the rabbit Achilles and flexor digitorum superficialis tendons and the appearance of the tendons, which were well demonstrated on MR imaging but poorly characterized on US images.

In rabbit, the medial head of the gastrocnemius muscle takes origin from the popliteal surface of the femur proximal to the medial condyle, whereas the lateral head arises from the lateral femoral condyle and joins the soleus tendon distally.[4] We found that the 2 distinct gastrocnemius tendons fused at 93% of their course, close to the calcaneal insertion. This finding is quite different from human anatomy, where the tendons of the medial and lateral heads of the gastrocnemius muscle converge more proximally, at 23% of their course in our human specimen, to form the Achilles tendon.[19,23] The imaging of the human Achilles specimen in this study depicts normal anatomy, as previously documented.[11,16]

We also document the lateral rotation of the medial gastrocnemius tendon in rabbit as it tracks distally, where it is positioned posterior to the lateral gastrocnemius tendon. This rotation seems equivalent to the spiral arrangement of collagen fibers within human Achilles tendons: as the human Achilles tendon descends, the fibers rotate externally approximately 90 degrees.[1] The rotational arrangement of the 2 gastrocnemius tendons may allow some elongation and elastic recoil, which helps the Achilles tendon store energy.

The flexor digitorum superficialis muscle in rabbits, corresponding to the flexor digitorum longus muscle in humans, arises from the middle half of the posterior surface of the tibia.[4] As the flexor digitorum superficialis tracks distally, it rotates laterally and is positioned posteriorly in relationship to the Achilles tendon. This anatomical position is quite different from that of the flexor digitorum longus in human, which runs behind the medial malleolus.[19,23] In rabbits, the flexor digitorum superficialis glides on the Achilles tendon–calcaneus junction. This anatomical characteristic is reminiscent of the flexor digitorum longus in human, which glides on the flexor hallucis longus tendon and which in the foot divides into 4 parts that typically insert into the lateral 4 distal phalanges.[19,23]

Additional anatomic features in rabbits should be considered. At the midpart of the Achilles tendon, approximately 15 mm proximal to the Achilles tendon–calcaneus insertion, the 2 gastrocnemius head tendons are seen distinctly, and the flexor digitorum superficialis tendon is comparable in size to either the medial or lateral gastrocnemius tendon and shares the same fascia. Some studies report mechanical testing of the rabbit Achilles tendon but fail to report isolation of the flexor digitorum superficialis tendon.[6,14,29,30] Different treatment of the flexor digitorum superficialis tendon at the time of testing may explain the large variations in mechanical strength previously reported.[14,29,30]

MR imaging of the rabbit Achilles tendon in the cross-sectional plane at 3-mm intervals allows for detailed views that match the particular relationships found on gross cross-section anatomy. Sagittal images at 2-mm intervals were less helpful, and this drawback can be explained by the small dimension of the tendons and the rotation of tendons with respect to the anteroposterior plane as one tracks from the proximal to distal aspect of the tendons. Particular attention and care could be made to create oblique–sagittal MR views of these tendons on image acquisition; doing so might improve tendon visualization in a longitudinal axis. Only 2 studies have previously imaged the rabbit Achilles tendon using MR imaging, and they did not comment on particular anatomic relationships.[6,28] Blaiser and White[6] imaged the rabbit hindlimb in the coronal and sagittal planes without axial sections. As we have shown in this study, the anatomy is most clearly demonstrated in the axial plane. Seo and colleagues[28] did acquire images in the axial plane but do not describe the 2 separate gastrocnemius tendons and relatively short Achilles tendon and, although they identified the flexor digitorum superficialis tendon, they did not elaborate on its relation to the Achilles tendon.

The normal sonographic appearance of a tendon depends upon the incident beam being perpendicular to the tendon.[20] Anisotropy causes a reduction in tendon echogenicity with only subtle modifications in the incident beam angle,[10] and this artifact can be mistaken for underlying disease and tendinosis.[7] The difficulty with the US examination of the rabbit Achilles tendon in our study was due to the small size of all 3 tendons and the different courses of these tendons of the hindlimb, the medial and lateral gastrocnemius and flexor digitorum superficialis. Indeed, previous US studies of the rabbit Achilles tendon[22,25] obtained similar size measurements to those found in our series, but they do not depict any anatomic detail present in the hindlimb. In addition, any measurements obtained in those earlier studies may reflect several tendons, depending at which level the measurement is taken. The unique anatomy of the rabbit Achilles tendon, its 2 major contributors, and its proximity to the prominent flexor digitorum superficialis tendon cause particular technical difficulties on US examination. We therefore do not recommend US examination for tracking of the Achilles in this model.

There are possible limitations to the study design that we wish to address. We assumed that freezing and thawing of the specimens did not alter the anatomic relations around the Achilles tendon. In addition, measures could be reported as cross-sectional area, although we believe the correlation between anteroposterior dimension and cross-sectional area in these round tendons support our conclusions. Finally, future studies could investigate tendon size at multiple levels.

In conclusion, the gross and imaging anatomy of the rabbit Achilles tendon differ from those of the human tendon: the lateral and medial gastrocnemius tendon fibers merge into the Achilles tendon very distally, the contribution of the soleus is negligible, and a large flexor digitorum superficialis tendon within the Achilles tendon sheath rotates dorsally and laterally and runs posterior to the Achilles tendon–calcaneus insertion. These peculiarities must be considered when using the rabbit Achilles tendon as a research model. Generalization of research results to human Achilles tendon disease hinges on proper consideration of these anatomic and imaging features.

Acknowledgments

This study was supported by the Workplace Safety and Insurance Board of Ontario and the Canadian Institutes of Health Research. We thank Hossein M Yazdi, MD (Department of Pathology and Laboratory Medicine, Ottawa Hospital, Canada) and Nanthan Ramachandran (Bone and Joint Research Laboratory, University of Ottawa, Canada) for their help in obtaining the gross cross-section images, Eric Murray and Josianne Dodier (both of the Department of Radiology, Ottawa Hospital, Canada) for their MRI and US expertise, respectively, and Julie Courchesne for specimen preparation.

References

1. **Alexander RM, Bennet-Clark HC.** 1977. Storage of elastic strain energy in muscle and other tissues. Nature **265:**114–117.
2. **Archambault JM, Hart DA, Herzog W.** 2001. Response of rabbit Achilles tendon to chronic repetitive loading. Connect Tissue Res **42:**13–23.
3. **Backman C, Boquist L, Fridén J, Lorentzon R, Toolanen G.** 1990. Chronic Achilles tendinosis: an experimental model in the rabbit. J Ortho Res **8:**541–547.
4. **Barone R, Pavaux C, Blin PC, Cuq P.** 1973. Plane 52. In: Mornet P, editor. Atlas d'anatomie du lapin. Paris: Masson & Cie. p 61–63.
5. **Benazzo F, Stennardo G, Mosconi M, Zanon G, Maffulli N.** 2001. Muscle transplant in the rabbit's Achilles tendon. Med Sci Sports Med **33:**696–701.
6. **Blaiser RD, White R.** 1998. Duration of immobilization after percutaneous sliding heel–cord lengthening. J Ped Ortho **18:**299–303.
7. **Crass JR, van de Vegte GL, Harkavy LA.** 1988. Tendon echogenicity: ex vivo study. Radiology **167:**499–501.

8. **Crum JA, LaPrade RF, Wentorf FA.** 2003. The anatomy of the posterolateral aspect of the knee. J Ortho Res **21:**723–729.
9. **Cunha AD, Parizotto NA, Vidal BC.** 2001. The effect of therapeutic ultrasound on repair of the Achilles tendon (tendo calcaneus) of the rat. Ultrasound Med Biol **27:**1691–1696.
10. **Dussik KT, Fritch DJ, Kyriazidou M, Sear RS.** 1958. Measurements of articular tissues with ultrasound. Am J Phys Med **37:**160–165.
11. **Ferkel RD, Flannigan BD, Elkins BS.** 1991. Magnetic resonance imaging of the foot and ankle: correlation of normal anatomy with pathologic conditions. J Foot Ankle **11:**289–305.
12. **Han S, Gemmell SJ, Helmer KG, Grigg P, Wellen JW, Hoffman AH, Sotak CH.** 2000. Changes in ADC caused by tensile loading of rabbit Achilles tendon: evidence of water transport. J Magn Res **144:**217–227.
13. **Jahnke AH Jr, Messenger MT, Patterson JD.** 1999. Common ankle injuries. In: Lillegard WA, Butcher JD, Rucker KS, editors. Handbook of sports medicine: a symptom-oriented approach, 2nd ed. Woburn (MA): Butterworth–Heinemann. p 1000–2000.
14. **Jassem M, Rose AT, Meister K, Indelicato PA, Wheeler D.** 2001. Biomechanical analysis of the effect of varying suture pitch in tendon graft fixation. Am J Sports Med **29:**734–737.
15. **Kesava Reddy G, Stehno-Bittel L, Enwemeka CS.** 1998. Laser photostimulation of collagen production in healing rabbit Achilles tendons. Laser Surg Med **22:**281–287.
16. **Kier R, Dietz MJ, McCarthy SM, Rudicel SA.** 1991. MR imaging of the normal ligaments and tendons of the ankle. J Comp Assist Tomogr **15:**477–482.
17. **Kramer M, Gerwing M, Michele U, Schimke E, Kindler S.** 2001. Ultrasonographic examination of injuries to the Achilles tendon in dogs and cats. J Sm Anim Pract **42:**531–535.
18. **Kuo PL, Li PC, Shun CT, Lai JS.** 1999. Strain measurement of rabbit Achilles tendons by ultrasound. Ultra Med Biol **25:**1241–1250.
19. **Leeson CR, Leeson TS.** 1989. Human structure. Toronto: B.C. Decker.
20. **Madaras EI, Perez J, Sobel BE, Mottley JG, Miller JG.** 1988. Anisotropy of the ultrasonic backscatter of myocardial tissue: II. measurements in vivo. J Acoust Soc Am **83:**762–769.
21. **Matsumoto F, Trudel G, Uhthoff UK, Backman DS.** 2003. Mechanical effects of immobilization on the Achilles tendon. Arch Phys Med Rehab **84:**662–667.
22. **Noguchi M., Kitaura T, Ikoma K, Kusaka Y.** 2002. A method of in-vitro measurement of the cross-sectional area of soft tissues, using ultrasonography. J Orthop Sci **7:**247–251.
23. **Palastanga N, Field D, Soames R.** 1998. Anatomy and human movement, 3rd ed. Oxford: Butterworth–Heinemann. p 1000–2000.
24. **Popesko P, Rajtová V, Horák J.** 1990. Colour atlas of the anatomy of small laboratory animals. Volume 1, Rabbit and guinea pig. London: Wolfe Publishing. p 129–143.
25. **Rompe JD, Kirkpatrick CJ, Kullmer K, Schwitalle M, Krischek O.** 1998. Dose-related effects of shock waves on rabbit tendo Achillis. A sonographic and histological study. J Bone Joint Surg Br **80:**546–552.
26. **Saini NS, Roy KS, Bansal PS, Singh B, Simran PS.** 2002. A preliminary study on the effect of ultrasound therapy on the healing of surgically severed Achilles tendons in five dogs. J Vet Med **49:**321–328.
27. **Schepsis AA, Jones H, Haas AL.** 2002. Achilles tendon disorders in athletes. Am J Sports Med **30:**287–305.
28. **Seo Y, Ikoma K, Takamiya H, Kusaka Y, Tsoref L, Eliav U, Shinar H, Navon G.** 1999. 1 H double-quantum-filtered MR imaging as a new tool for assessment of healing of the ruptured Achilles tendon. Magn Reson Med **42:**884–889.
29. **Thermann H, Frerichs O, Biewener A, Krettek C.** 2001. Healing of the Achilles tendon: an experimental study. Foot Ankle Int **22:**478–483.
30. **Yasuda T, Kinoshita M, Abe M, Shibayama Y.** 2000. Unfavorable effect of knee immobilization on Achilles tendon healing in rabbits. Acta Ortho Scand **71:**69–73.